

~~FAX COVER PAGE~~

MASSACHUSETTS INSTITUTE OF TECHNOLOGY
 LIGO Project, Room 20B 145, 18 Vassar Street, Cambridge, MA 02139
 617-253-4824, Fax 617-253-7014

TO:	Stan Whitcomb
ORGANIZATION:	LIGO at CALTECH
FAX NUMBER:	
VOICE NUMBER:	
DATE:	January 5, 1996
TIME:	11:50AM

FROM:	David Shoemaker
ORGANIZATION:	LIGO at MIT
FAX NUMBER:	
VOICE NUMBER:	
REFER TO:	L160-7960001-COR
SUBJECT:	

NUMBER OF PAGES FAXED INCLUDING THIS COVER SHEET:	16
--	----

NOTE:

Sapphire Beamsplitters and Test Masses for Advanced Laser Interferometer Gravitational Wave Detectors

L. Ju, M. Notcutt, D. Blair, F. Bondu* and C. N. Zhao

Department of Physics, University of Western Australia
Nedlands, W.A. 6907, Australia

*Groupe VIRGO, Laboratoire de l'Accélérateur Linéaire,
CNRS-IN2P3, Université de Paris-Sud, F-91405 Orsay, France

Abstract

In this paper we present studies of the expected performance of a sapphire beamsplitter and test masses in a laser interferometer gravitational wave detectors. The internal thermal noise of a sapphire test mass is calculated compared with a silica test mass. Suspension system which will maintain high internal and pendulum Q-factors is discussed. The optical losses in a sapphire test mass are discussed and the orientation requirements on sapphire optical components due to birefringence are analysed. Results show that the noise floor of the interferometer due to internal thermal noise of test mass are - 16 times smaller for a sapphire test masses than silica test masses. Rayleigh scattering losses will set a limit to the recycling factors attainable if stress induced birefringence effect can be avoided.

1. INTRODUCTION

Laser interferometer gravitational wave detectors without resonant cavities in their arms but with very large power recycling gain and signal recycling gain [1, 2, 3] can be considerably simpler than the implementation of recycling in a Fabry-Perot Michelson as currently planned by the LIGO [4] and VIRGO [5] projects. High dual recycling gain can compensate for the absence of Fabry-Perot cavities in the arms.

In this scheme the full resonant enhanced light power (carrier) must be transmitted through the beamsplitter. Therefore the beamsplitter becomes a critical component of the system, with full sensitivity to seismic and thermal noise. The optical scattering, optical absorption and thermal lensing [6] become the critical limitations on performance.

It is well known that the thermal and mechanical properties of sapphire make it an interesting material for use in test masses. The combination of its very high Young's modulus, high thermal conductivity and low acoustic loss means that thermal lensing can be minimised while internal resonant modes have high frequency and low thermal noise. Single crystal cylinders of 200 - 300 mm diameter and similar length are commercially available.

Until recently it was not known whether good optical super polishing could be achieved on sapphire. Now excellent results from polishing [7] and the absence of coating problems [8] seem to indicate that the material is useable from this perspective. Recent measurements [9] have also shown that the optical absorption coefficient can be as low as 3 ppm/cm in sapphire samples at 1 μm wavelength. This is superior to most samples of fused silica. However several uncertainties remain before sapphire can be used with confidence in a laser interferometer.

In this paper we consider further aspects of interferometer design using a sapphire beamsplitter and end mirrors. We compare the thermal noise of a practical sapphire test mass with a similar silica test mass. We analyse methods of suspension of sapphire test masses to prevent degradation of the internal mode Q-factors, while obtaining very low pendulum losses. We analyse the orientation requirements on sapphire optical components (imposed by the intrinsic birefringence of sapphire).

Our conclusions are generally positive. We show that the internal thermal noise in a typical test mass is ~ 16 times lower than that of a similar silica mass. We show that a membrane suspension system can allow very high internal mode Q-factor to be achieved. Methods of bonding a membrane hinge to sapphire which should achieve this performance are discussed. However there is a trade off between internal mode Q, longitudinal suspension mode frequency and rocking frequency. To achieve a worst case internal mode Q equal to the highest observed Q-factor in sapphire at room temperature, ($Q > 10^8$ [10]), a membrane with a Q-factor of 10^5 is required.

Our analysis also shows that the orientation requirements on the sapphire crystal are within reasonable operational tolerances while our measurements show that as long as stress birefringence is avoided, adequate birefringence homogeneity can be achieved. Assuming an interferometer operating at 1 μm wavelength, Rayleigh scattering losses of almost 20 ppm/cm are difficult to avoid. A Total absorption loss of ~ 60 ppm can be anticipated in a sapphire beamsplitter, depending on the material thickness. The high Rayleigh scattering sets limits on the maximum recycling gain.

2. THERMAL NOISE OF A SAPPHIRE TEST MASS

2.1 Internal modes

According to the fluctuation-dissipation theorem [11], the thermal noise due to the internal resonant of the test mass can be expressed by [12]

$$\Delta x^2 = \frac{4k_B T}{\omega} \sum_i \frac{\Phi_i(\omega_i) \omega_i^2}{M_i [(\omega_i^2 - \omega^2)^2 + \Phi_i^2(\omega) \omega^4]} \quad (1)$$

where ω_i and M_i are the angular frequency and the equivalent mass of the i^{th} mode respectively. Here the structural damping mechanism is assumed, with loss factor $\Phi(\omega) = 1/Q_i$, constant over a large frequency range [13, 14]. For frequencies $\omega \ll \omega_i$, the thermal noise can be expressed as

$$\Delta x^2 = \frac{4k_B T}{\omega} \Phi(\omega) \sum_i \frac{1}{M_i \omega_i^2} = \frac{4k_B T}{\omega} \frac{\Phi(\omega)}{M_{eq} \omega_{eq}^2} \quad (2)$$

The internal resonant modes of a sapphire test mass can be calculated by numerical methods [15, 16, 17] based on the theory of elasticity in continuous media. We have assumed a free mass model and used the program "CYPRES" [16] to calculate various test mass configurations. For a cylindrical sapphire test mass with diameter of $d = 200$ mm and thickness of $H = 200$ mm (≈ 25 kg), the first 9 internal resonances below 60 kHz are listed in table I. The high internal resonant frequencies in the sapphire test mass are very important in reducing their thermal noise contribution. "CYPRES" allows the effective mass and frequency of the test mass normal modes to be calculated.

Table I

Mode number	frequency (Hz)	M_i (kg)	$M_i \omega_i^2$
0 0 1	22652	9.13	1.85×10^{11}
0 0 2	29284	17.8	6.04×10^{11}
0 0 3	36997	91.9	4.96×10^{12}
0 0 4	46468	2.45	2.09×10^{11}
0 0 5	54115	2.75	3.18×10^{11}
0 1 1	27480	20.7	6.17×10^{11}
0 1 2	34385	4.24	1.98×10^{11}
0 1 3	45411	8.33	6.78×10^{11}
0 1 5	52506	16.9	1.84×10^{12}

We tested for convergence of the thermal noise calculation by integrating over the first 200 normal modes, and compared the results with that of a silica test mass of the same dimensions. The values of $M_{eq}\omega_{eq}^2$ for sapphire and silica test masses of the same dimensions are 16.3×10^9 and 2.89×10^9 respectively. It can be seen that the value $M_{eq}\omega_{eq}^2$ of a sapphire test mass is 6.54 times greater than that of a silica test mass. The highest internal mode Q-factor reported in silica is 7×10^6 [18]. This compares with 3×10^8 reported for sapphire [10]. The reduced losses, combined with the increased values of $M_{eq}\omega_{eq}^2$ of sapphire means that the thermal noise amplitude of this sapphire test mass will be a factor of

$$\sqrt{\frac{Q_{sapp}(M_{eq}\omega_{eq}^2)_{sapp}}{Q_{silica}(M_{eq}\omega_{eq}^2)_{silica}}} = 16.7$$

times better than that of a silica test mass with the same dimensions.

In this analysis we have assumed that the incident laser light is concentric with the test mass. In reality it is advantageous to illuminate the test mass at the centre of percussion to reduce pendulum thermal noise contributions as discussed below. The offset of the beam will alter the integrated thermal noise by a small factor.

2.2 Pendulum thermal noise due to flexure elastic loss

It has been shown previously that a membrane flexure allows enhanced pendulum Q-factors [19, 20]. The advantage of using a short thin membrane flexure is that it has very high violin string modes and low flexural spring constant. A practical sapphire test mass suspension with a short membrane flexure is shown in figure 1. With the dimension given above, this compound pendulum will have a resonant frequency of 1.3 Hz. The centre of percussion of this pendulum, at which the transfer function will be the same as a simple pendulum, will be at 43 mm below the centre of mass.

Figure 2 shows the thermal noise due to internal resonances of the sapphire test masses given in previous section. Here we assume sapphire has a Q-factor of factor of 10^8 . Also in figure 2 is the thermal noise of the pendulum mode with a niobium membrane flexure with Nb having a Q-factor of 10^5 . At 10 Hz the noise is mainly pendulum mode thermal noise which reaches 4×10^{-16} m/ $\sqrt{\text{Hz}}$ level, while at 100 Hz the internal resonant modes thermal noise dominate at a level of $\sim 4 \times 10^{-18}$ m/ $\sqrt{\text{Hz}}$. The "violin string" modes of the short membrane are very high (~ 100 kHz), leaving a "clean window" for gravitational wave detection.

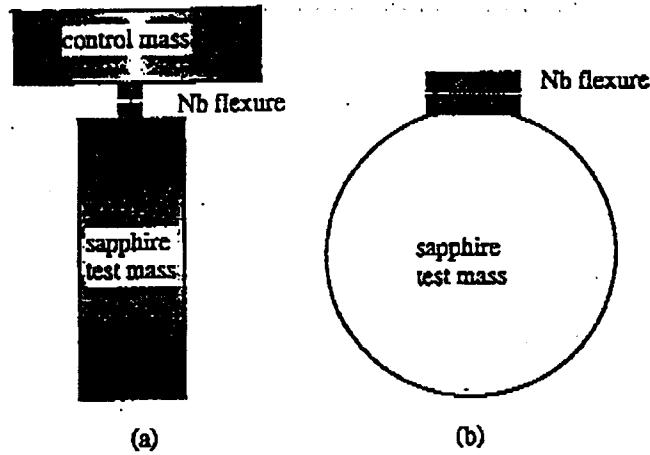


Fig. 1. A practical design for a sapphire beamsplitter. (a) side view; (b) front view. The suspension element is a thin niobium membrane flexure, typically 25 μm thick, 2 mm long and 4 cm wide.

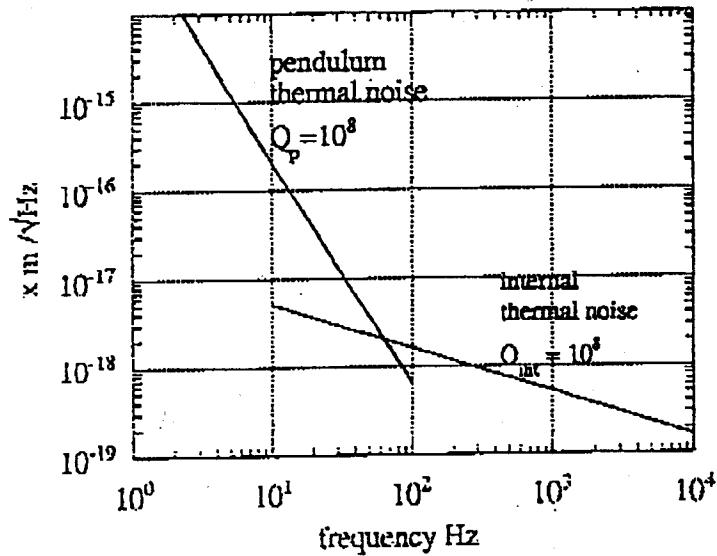


Fig. 2. Predicted thermal noise of a sapphire test mass. The intrinsic Q-factor of the test mass is chosen as 10^4 . The pendulum Q factor is chosen as 10^9 with a Nb membrane flexure Q-factor of 10^5 .

2.3. Bonding of the flexure to the test mass

It is well known that imperfect clamping of mechanical components will cause excess acoustic losses. In particular the imperfect bonding of the flexure to the test mass will cause additional loss in the pendulum.

We propose the use of well established ceramic to metal sealing techniques to overcome this problem. Numerous methods have been developed for different applications [21]. Among these techniques, active metal seals, pressed diffusion seals and solder seals are of interest for our application. The refractory properties of niobium and sapphire, their satisfactory thermal expansion match from liquid helium temperature [22] to 2000 °C [23], and the low acoustic losses of both materials makes niobium appear ideally suited for bonding to sapphire for the purpose of creating a low loss flexure pivot suspension.

Sapphire to Nb seals using active metal brazing with titanium and vanadium allows very high strength bonding at ~ 1800 °C [23]. Active metal brazing alloys such as Incusil (Indium-copper-silver) and Cusil (Copper-silver) can create a high integrity bond at 700 - 860 °C [24].

We have preliminarily investigated direct diffusion bonding between sapphire and Nb at 1400 °C. Preliminary experiments have achieved yield strength ~ 15 MPa for joint created at a contact pressure of about 5 MPa. Higher strength joints can be expected using higher temperatures and surface pressure. It remains to determine whether such joints have low acoustic loss, and to compare the results with brazed joints.

3. THE EFFECT OF LOW Q-FACTOR UPPER STAGES ON SAPPHIRE TEST MASS INTERNAL Q-FACTOR

In practice a test mass will be suspended from a vibration isolation stack as shown in figure 1. Usually the intrinsic Q-factor of the isolator elements will be low. We assume here the use of metal cantilever spring vibration isolators [25] with normal mode Q-factors ~ 10^3 . Suppose the last isolation stage (control mass) has a mass of 40 kg and internal resonant frequency of the order 10^3 Hz. From section 1.1, the lowest internal resonant frequency of a 25 kg sapphire test mass can exceed 20 kHz. It is possible, however that the internal mode Q-factor of the test mass will be degraded through coupling to the internal mode of the control mass. Such Q-factor degradation will directly degrade the test mass thermal noise. To assess this problem, the system was modelled in one dimension, using lumped mass and spring elements [26]. Two models were considered. One consists of a directly coupled system, using a moderately low loss membrane hinge. The second consists of one in which a small cantilever stage is inserted between the control mass and test mass to provide some degree of vertical isolation. Figures 3 and 4 show the two mechanical systems and their models (see the figure captions for full details).

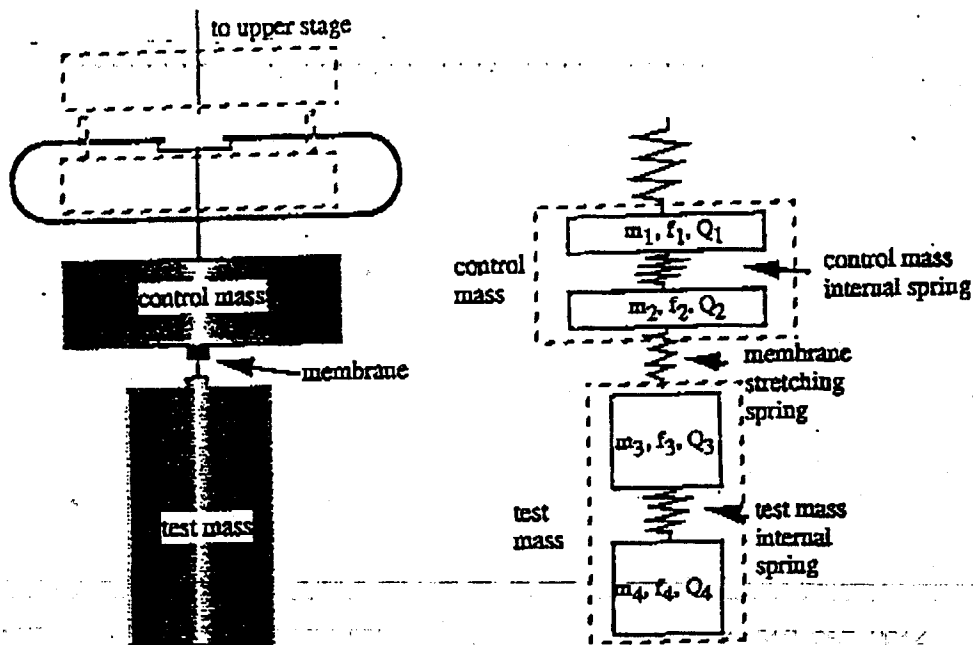


Fig 3. Model one: test mass suspended directly under control mass. A four stage spring mass model is used. Spring 1 -- spring of the whole isolator; spring 2 -- internal spring of the control mass; spring 3 -- test mass membrane flexure stretching spring; spring 4 -- equivalent test mass internal spring

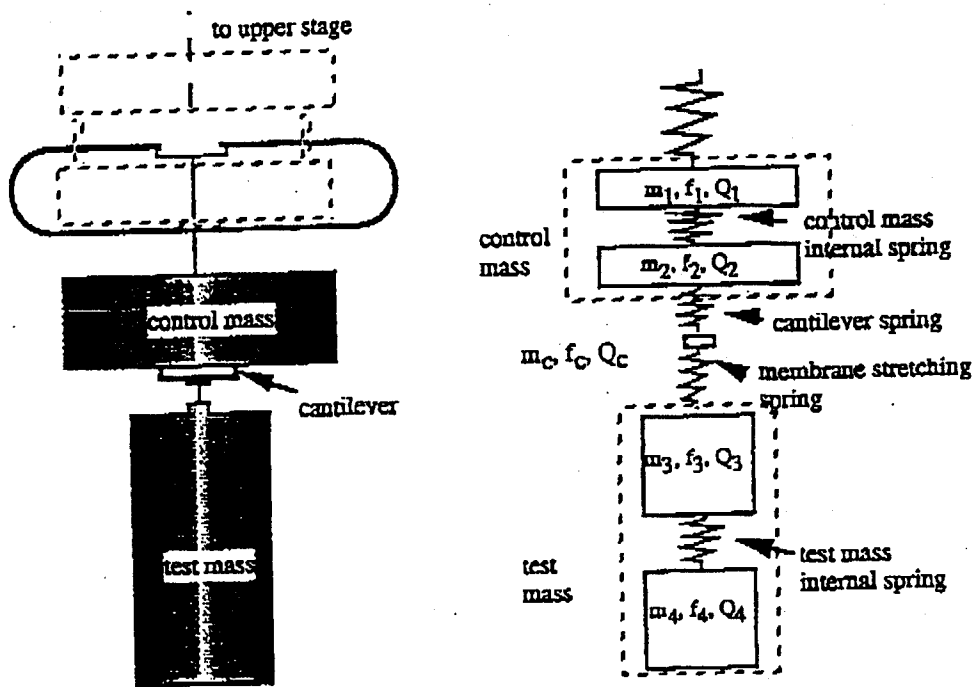


Fig. 4 Model 2: test mass suspended under a low loss, low mass cantilever which in turn is connected to the control mass. A five stage spring and mass model is used. Spring C --cantilever spring; the other elements are the same as in model 1.

To examine the effect of Q degradation of the test mass, we assume that the test mass has an extremely high intrinsic Q -factor ($Q = 10^{10}$). Other parameters of the model are

$$f_1 = 2 \text{ Hz}, f_2 = 10^3 \text{ Hz}, f_3 = 300 \text{ Hz}^*, f_4 = 10^4 \text{ Hz}, (f_c = 100 \text{ Hz});$$

$$m_1 = m_2 = 25 \text{ kg}, m_3 = m_4 = 12.5 \text{ kg}, (m_c = 0.1 \text{ kg});$$

$$Q_1 = 10^3, Q_2 = 10^3, Q_3 = 10^5, Q_4 = 10^{10} \text{ m } (Q_c = 10^5).$$

*The stretching mode frequency of the foil flexure f_3 is chosen for a membrane flexure length of 2 mm, width of 4 cm and thickness of 25 μm .

Using the above parameters, the test mass internal mode Q for 4 stages (without small cantilever) is 4.25×10^8 . With the small cantilever added, the test mass internal mode Q is (almost) independent of Q_2 and f_2 (the Q -factor and internal frequency of the control mass). It is also independent of Q_c and f_c (the cantilever stage Q -factor and frequency). The test mass internal mode Q is dependent on the mass of the cantilever stage (m_c), the frequency of the membrane stage (f_3), and, of course, on the Q -factor of membrane flexure Q_3 . The results are shown in figures 5 and 6.

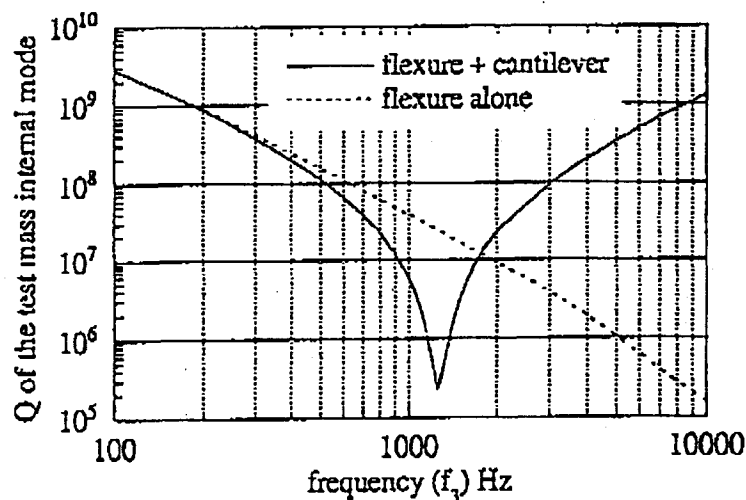


Fig. 5. Test mass internal resonant Q -factor as a function of the mass of the cantilever stage. The dotted line is that of a system without cantilever stage. It can be seen that the Q -factor of "flexure + cantilever" model exceeds that of "flexure alone" model only when the cantilever stage mass is impractically small.

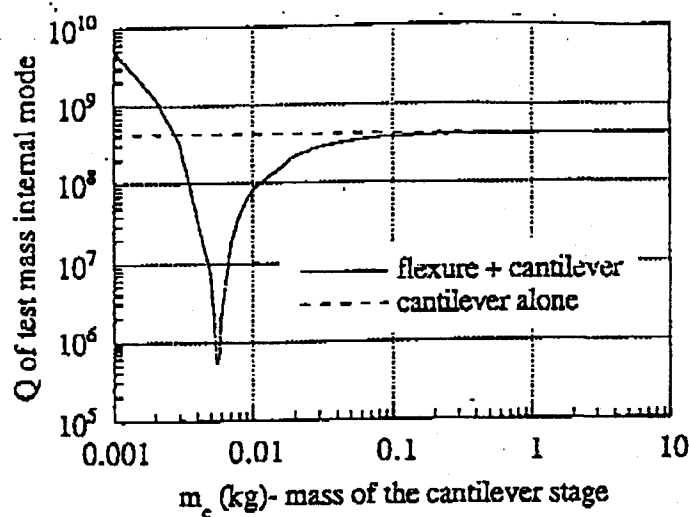


Fig. 6. Test mass internal resonant Q-factor as a function of the membrane flexure (with $f_3 = 300$ Hz).

In the model with a small cantilever intermediate stage, the anticipated Q enhancement of the intermediate stage can only be achieved for unrealistically low mass cantilevers. The test mass internal Q-factor is degraded strongly when the cantilever mass and membrane stretching frequency create a resonant coupling of energy from the test mass to the control mass. Therefore we conclude that in our case there is no advantage in adding a low mass stage in between the test mass and the control mass.

The high internal mode Q-factor in the "flexure only" model indicates that an internal resonant mode Q-factor of 10^8 of the sapphire test mass could be expected in the isolation and suspension system, assuming that the intrinsic Q-factor of the sapphire material is as reported in the literature^[10].

4. OPTICAL LOSSES IN SAPPHIRE

Having considered the mechanical properties of the suspension of sapphire test masses, we now discuss the optical characteristics of sapphire mirrors and beamsplitter.

5.1 Absorption

In a recycling interferometer, the full resonant power must pass through the beamsplitter. It is crucial that optical absorption of the beamsplitter is small to keep power losses small and minimise thermal lensing by the beamsplitter. Recent tests on sapphire have shown an absorption coefficient of $\alpha \sim 3$ ppm/cm at $1 \mu\text{m}$ [9]. With a thickness of 20 cm, the absorption

of a sapphire beamsplitter will be -60 ppm. With such a small thermal absorption and high thermal conductivity of sapphire, the thermal lensing of the sapphire beamsplitter will be small.

5.2 Rayleigh Scattering

Apart from the thermal absorption, there is an additional optical loss by scattering due to density fluctuation. The reduction in intensity should be written as

$$I = I_0 e^{-(\alpha + \gamma)x},$$

where γ is the scattering coefficient.

Detailed calculation using a computer program "OPTIMATR" gives a Rayleigh scattering limit for sapphire (o - ray at room temperature) of $\gamma = 18$ ppm/cm at $1 \mu\text{m}$ [27]. It can be seen that the Rayleigh scattering loss is much greater than the absorption loss and thus sets the limit to the achievable power recycling. However, the Rayleigh scattering does not contribute to thermal lensing.

5.3. Effects of Sapphire Birefringence for Beamsplitters

The intrinsic birefringence property of sapphire is one disadvantage. For perfect alignment the polarisation axis of the light will be aligned with one of the sapphire crystal's axes of symmetry. Relative misalignment of the polarisation and crystal axes will cause the light to become elliptically polarised as it travels through the sapphire. Misalignment may be caused by fluctuations of the beam or motion of the beamsplitter. From our experience of isolation systems for interferometers, this motion is likely to be the residual normal mode motion of rocking and rotation after electronic damping. In our system these motions have angular magnitudes a few microradians.

Sapphire is a uni-axial crystal with a c -axis of rotational symmetry. A number of combinations of polarisation, beam direction and c -axis alignment are possible. We have chosen the polarisation (e) to be parallel to the c -axis (c) and the propagation to be in the a -axis plane. Suppose the polarisation of the light (e) has a small angle ψ with the c -axis as shown in figure 7, the ellipticity introduced to the beam that double-passes the beamsplitter will lead to imperfect interference. The non-interfered light escapes from the interferometer out of each output port. In a power-recycled interferometer power loss is detrimental to the performance of the system as it limits the power enhancement by resonant reflection of the bright output. For this reason we investigate the losses caused by birefringence in a sapphire beamsplitter.

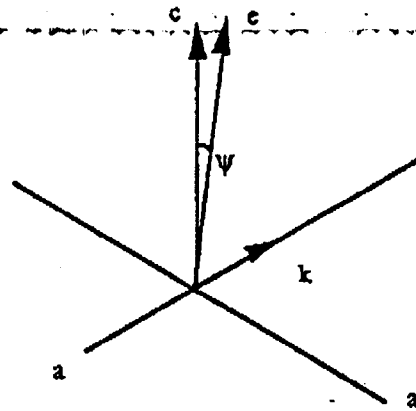


Fig. 7. Illustration of light polarisation direction in relation to sapphire axis.

The fraction of lost power is :

$$\frac{P_{lost}}{P} = \sin^2 \phi \sin^2 2\psi ,$$

where ψ is the angle between c and e , and 2ϕ is the difference in the phase shift of the light along the orthogonal crystal axes. For sapphire and laser light of $\lambda = 1064$ nm, the phase shift will be

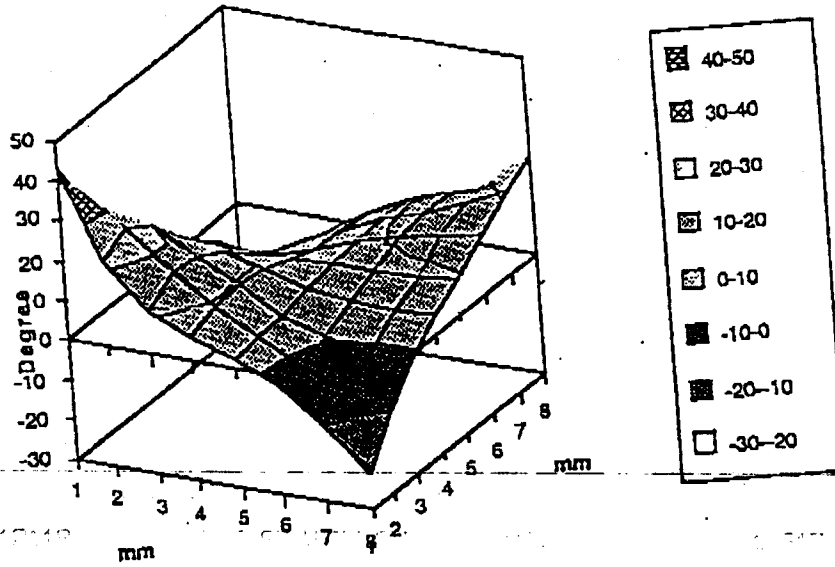
$$\phi = 2\pi / 270\mu m.$$

Since this is such a quickly varying function it will be set to it's maximum value, 1. Then

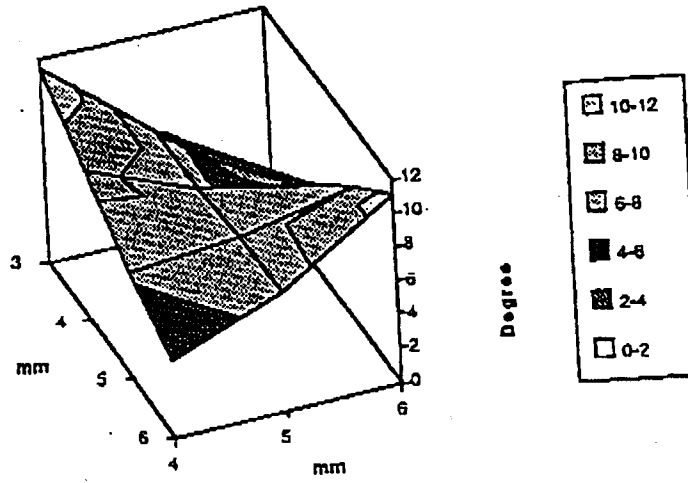
$$\frac{P_{lost}}{P} = \sin^2 2\psi = 4\psi^2.$$

For angles less than $100 \mu rad$, which is easy to realise in our suspension systems, this loss will be significantly less than other loss sources such as mirror losses and curvature mismatch. We conclude that the birefringence of sapphire is not a detrimental factor in using it as a beamsplitter substrate.

On the other hand, the inhomogeneity of sapphire and stress in it can cause birefringence. We have investigated birefringence of a small $10 \times 10 \times 25$ mm³ sapphire sample, using a similar method to that of Logan *et. al.* [28], which consisted of a half-wave plate, polariser and a phase compensator. The observed phase shift between the ordinary ray and extraordinary ray due to birefringence is shown in figure 8 (a). The sapphire sample shows stable performance in the central unstrained region and degraded at corners where high stress is expected. The phase shift in the centre is within 2° ($6^\circ - 8^\circ$) as shown in figure 8 (b).



(a)



(b)

Fig. 8 Phase shift map of the ordinary ray and extraordinary ray in the sapphire sample due to birefringence.

(a) map of the whole piece; (b) enlarged central area.

Because the alignment between the incident light polarisation and c axis of the sapphire sample is not very accurate in this measurement, there is a fundamental phase shift which can be reduced by better alignment. Secondly, this sapphire sample is rather small. It is highly possible that the edge stress effect penetrate all the way to the central part.

For a large piece of sapphire with dimension of the order $20 \times 20 \times 20 \text{ cm}^3$, the stress at the centre is expected much smaller. If assuming the average loss in the mirrors to be the order of 10^{-5} per mirror [28], the total mirror loss would be $\sim 10^{-3}$ for 100 bounces of light in one arm. Should the loss due to inhomogeneous birefringence effect be of the same order of or less than other mirror losses, the inhomogeneous birefringence phase shift should be smaller than 2° in a beamsplitter. Further more accurate measurements on large sapphire samples are needed to confirm these results.

6. CONCLUSION

Sapphire with its excellent mechanical and thermal properties is an attractive material to use for beamsplitter and test masses in laser interferometer gravitational wave detectors. We have shown that the birefringence of sapphire should not be a problem with our well controlled vibration isolation and suspension systems. However, the birefringence induced by stress and inhomogeneity in a large piece of sapphire need further investigation to confirm that the phase shift is small.

The internal thermal noise amplitude of a sapphire test mass will be ~ 16 times better than that of a fused silica test mass with the same dimensions. The end-supported beamsplitter will have its fundamental longitudinal mode most severely degraded by the suspension system. The model used here therefore represents the worst case Q -degradation of the beamsplitter. A longitudinal frequency of 300 Hz, corresponds to a membrane of only one or two millimetres length. The results show that the test mass can maintain a Q -factor $\sim 10^8$ when suspended in this way.

Further work is required to confirm the practicality of the proposed suspension systems discussed here, and to determine whether large sapphire samples maintain the optical performance observed in small scale samples. If this work is confirmed and realised, it means that the total local noise sources in laser interferometers can be reduced by a factor ~ 16 . This means that there is a substantial margin for creating optical readout systems capable of achieving this sensitivity advantage, for example, by using narrow band resonant recycling schemes. In particular it means that laser interferometer gravitational wave detectors can be reduce in size by

more than an order of magnitude while maintaining the sensitivity predicted using silica test masses. Conversely, the 3 - 4 km interferometers currently under construction can be enhanced in sensitivity by a similar margin. In both cases the uncertainty principle sets a fundamental limit which is uncomfortably close to the practical limits discussed here.

ACKNOWLEDGMENT

We would like to thank Crystal Systems for providing sapphire samples for absorption tests. We also like to thank John Winterflood in helping on Q modelling program.

REFERENCES

1. R. P. Drever, "Interferometric detectors of gravitational radiation", in *Gravitational Radiation*, eds. N. Deruelle and T. Piran, North-Holland Publishing, (1983).
2. B. J. Meers, "Recycling in laser interferometric gravitational wave detectors", *Phys. Rev. D* **38**, 2317, (1988).
3. B. J. Meers and K. A. Strain, "An experimental demonstration of dual recycling for interferometric gravitational-wave detectors", *Phys. Rev. Lett.*, **66**, 1391 (1991).
4. A. Abramovici, W. E. Althouse, R. W. P. Drever, Y. Gürsel, S. Kawamura, F. J. Raab, D. Shoemaker, L. Sievers, R. E. Spero, K. S. Thorne, R. E. Vogt, R. Weiss, S. E. Whitcomb and M. E. Zucker, (1992). "LIGO: The laser interferometer gravitational-wave observatory", *Science*, **256**, 325.
5. B. Mours, (1993). "The VIRGO project", Contribution to the Europhysics Conference on High Energy Physics.
6. W. Winkler, K. Danzmann, A. Rüdiger and R. Schilling, "Heating by optical absorption and the performance of interferometric gravitational wave detectors", *Phys. Rev. A*, **44**, 7022 (1991).
7. C. Walsh and A. Leistner, CSIRO Division of Applied Physics, Lindfield, private communications, 1995.
8. J.-M. Makowski, Institut de Physique Nucleaire, Université Claude Bernard, Lyon, France, private communications, 1995.
9. D. G. Blair, F. Cleva and N. Mang, "Optical absorption measurements in monocrystalline sapphire at 1micron", submitted to *Optical Materials*, (1995).
10. V. B. Braginsky, V. P. Mitrofanov and O. I. Panov, *Systems with Small Dissipation*, University of Chicago Press, 1985.
11. H. B. Callen and T. A. Welton, *Phys. Rev.*, **83**, 34 (1951).

12. P. R. Saulson, "Thermal noise in mechanical experiments", *Phys. Rev. D*, **42**, 2437 (1990).
13. P. R. Saulson, R. T. Stebbins, G. D. Dumont and S. E. Mock, "The inverted pendulum as a probe of anelasticity", *Rev. Sci. Instrum.*, **65**, 182 (1994).
14. A. Gillespie and F. Raab, "Thermal noise in the test mass suspensions of a laser interferometer gravitational-wave detector prototype", *Phys. Lett. A*, **178**, 357 (1993).
15. A. E. M. Love, *A treatise on the mathematical theory of elasticity*, Dover, New York, 1944.
16. F. Bondu, J. Y. Vinet, "Mirror thermal noise in interferometric gravitational-wave detectors", *Phys. Lett. A*, **198**, 74 (1995).
17. A. Gillespie and G. Raab, "Thermally excited vibrations of the mirrors of laser interferometer gravitational-wave detectors", *Phys. Rev.*, **52**, 577, (1995).
18. V. B. Braginsky, V. P. Mitrofanov and O. A. Okhrimenko, "Oscillators for free-mass gravitational antennas", *JETP Lett.*, **55**, 432 (1992).
19. W. Martin, *Experiments and Techniques for the Detection of Gravitational and Pulsed Electromagnetic Radiation from Astrophysical Sources*, Ph. D Thesis, Universit of Glasgow, 1987.
20. D. G. Blair, L. Ju and M. Notcutt, "Ultrahigh Q pendulum suspensions for gravitational wave detectors", *Rev. Sci. Instrum.*, **64**, 1899 (1993)
21. W. H. Kchi, *Handbook of Materials and Techniques for Vacuum Devices*, Reinhold Publishing Co., USA, 1967.
22. P. Vietch,
23. L. Bogart and I. Ben-Zvi, "A sapphire to niobium vacuum seal for the temperature range 2 - 2000 K", *Rev. Sci. Instrum.*, **45**, 713 (1974).
24. WESGO Technical Ceramics and Brazing Alloys, Technical Data, 1995.
25. L. Ju and D. G. Blair, "Low resonant frequency cantilever spring vibration isolator for gravitational wave detectors", *Rev. Sci., Instrum.*, **65**, 3482 (1994).
26. M. E. Tobar, "Characterizing multi-mode resonant-mass gravitational wave detectors", *Phys. D: Appl. Phys.*, **28**, 1728 (1995).
27. Crystal Systems, Private communications, 1995, which referenced W. J. Tropf and M. E. Thomas at The Johns Hopkins University.
28. J. E. Logan, N. A. Robertson, J. Hough, "Measurements of birefringence in a suspended sample of fused silica", *Opt. Comm.*, **107**, 342 (1994).